Programmable soft robotics actuator with pneumatic networks (PneuNets)

Hadi, Y. W., Sunarya, B. A. Y., Alifdhyatra, A. F., Hidayat, E., Salomo, J., Purwidyantri, A., Prabowo, B. A., & Anshori, I. (2023). Programmable soft robotics actuator with pneumatic networks (PneuNets). *IEEE Sensors Journal*, *23*(17), 19382-19389. https://doi.org/10.1109/JSEN.2023.3297402

Published in:
IEEE Sensors Journal

Document Version:
Peer reviewed version

Queen's University Belfast - Research Portal:
Link to publication record in Queen's University Belfast Research Portal

Publisher rights
© 2023 IEEE.
This work is made available online in accordance with the publisher's policies. Please refer to any applicable terms of use of the publisher.

General rights
Copyright for the publications made accessible via the Queen's University Belfast Research Portal is retained by the author(s) and / or other copyright owners and it is a condition of accessing these publications that users recognise and abide by the legal requirements associated with these rights.

Take down policy
The Research Portal is Queen's institutional repository that provides access to Queen's research output. Every effort has been made to ensure that content in the Research Portal does not infringe any person's rights, or applicable UK laws. If you discover content in the Research Portal that you believe breaches copyright or violates any law, please contact openaccess@qub.ac.uk.

Open Access
This research has been made openly available by Queen's academics and its Open Research team. We would love to hear how access to this research benefits you. – Share your feedback with us: http://go.qub.ac.uk/oa-feedback

Download date:17. Mar. 2025

Programmable Soft Robotics Actuator with Pneumatic Networks (PneuNets)

Yulyan Wahyu Hadi, Member, IEEE, Basilius Agung Yason Sunarya, Athar Fadlankahlil Alifdhyatra, Egi Hidayat, Member, IEEE, Jonathan Salomo, Agnes Purwidyantri, Briliant Adhi Prabowo, Member, IEEE, and Isa Anshori, Member, IEEE.

***Abstract*—In this paper, we studied pneumatic networks (PneuNets) platform fabrication and evaluated the effect of variations in design parameters and inextensible layer materials on the bending angle of PneuNets. We also developed a pneumatically driven soft robot that required pressurized gas to move according to its function. A programmable pneumatic pump circuit comprising a direct current (DC) air pump and valves connected with tubes was used to actuate the platform and control the internal pressure. Two control methods were tested: a straightforward on-off control and a proportional-integral (PI) control based on a linear model derived from system identification. Comparisons for input tracking performance were made, with on-off control providing a better error performance than PI control, producing an oscillation of 2 kPa along the reference input. The results of parameter variations of PneuNets designs conclude the strategies to obtain a larger bending angle: thinner inner chamber walls, lengthened size of the PneuNets, increased number of chambers, and a smaller grammage and thickness of the inextensible layer.**

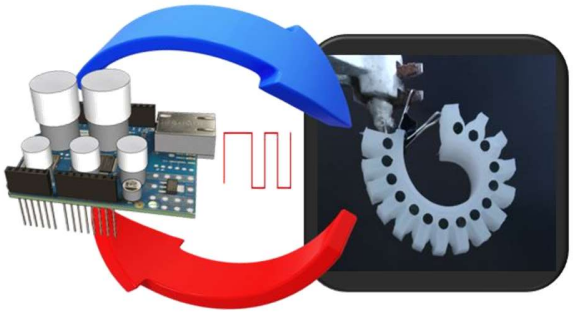

***Index Terms*— Extensible layer, Inextensible layer, Soft robotics, Pressure control, Pneumatic pump.**

I. Introduction

One of the pivotal milestones in robotics evolution is lightweight robots, which can be deformed and interact with humans, known as 'soft robots', inspired by structural properties similar to and found in nature [1]. The materials used in building up a robotic system create the critical distinction between hard and soft robots. Hard robots are made of rigid structural materials with several arms and axes; while soft robots are made of soft, stretchable, and reversible materials [2], [3]. The application of soft robotics with soft materials in robotics has been captivating since it enables robots with softer interactions between humans and machines toward potential applications in the biomedical field[4]. For example, robots that operate inside the human body in surgery and endoscopy. Other applications include rehabilitation, help, and prosthetics to replace limbs or artificial organs. Fluidic Elastomer Actuator (FEA) is a type of actuator for soft robots with high elongation value, adaptability, and low power [5]. The FEA comprises a synthetic elastomer operated by the actuator's expansion under pressure, either pneumatically or hydraulically. Pneumatic FEA has the advantages of having air available everywhere, being environmentally friendly, lightweight, and having low viscosity [6]. Pneumatic networks (PneuNets) systems are widely used in soft robotics by designing chambers on polymer elastomers and pneumatic actuation that can change the shape of the actuator body in a controlled manner [7]. The effect of material properties and chamber geometry on the movement of PneuNets is generated by pressure, and its configuration is determined by the channel structure [8]. The PneuNets movement depends on their design, leading to significant deflections, and it is the potential for medical applications, particularly for prosthetic and rehabilitation devices.

The actuation method for soft robots is also different from conventional robotics. Depending on the design, it can be actuated with cables, fluid, or electroactive polymer [6], [9]. In a pneumatic-based soft robot, a method to deliver airflow toward the soft robot actuator uses gas to generate the pressure needed to deform the soft robotics body. Even though gas in pneumatic actuation is lightweight, has low viscosity, and is readily available, it requires complex to control because of its compressibility [10], [11]. Pumps, regulators, or valves are typically applied to deliver gas with pressure into the soft body. Marchese et al. reported the pressure generated by a custom fluidic drive cylinder operated by a digital signal to control the

Yulyan Wahyu Hadi, Athar Fadlankahlil Alifdhyatra, and Egi Hidayat. are with the Control and Computer Systems Research Group, School of Electrical Engineering and Informatics, Bandung Institute of Technology.

Basilius Agung Yason Sunarya, Jonathan Salomo, and Isa Anshori are with Lab-on-Chip Laboratory, Biomedical Engineering Department, School of Electrical Engineering and Informatics, Bandung Institute of Technology.

Agnes Purwidyantri is with the School of Chemistry and Chemical Engineering, Queen's University Belfast, UK.

Briliant Adhi Prabowo is with the School of Mathematics and Physics, Queen's University Belfast, UK.

Yulyan Wahyu Hadi and Basilius Agung Yason Sunarya contributed equally.

Corresponding authors: Isa Anshori: isaa@staff.stei.itb.ac.id and Briliant Adhi Prabowo: b.prabowo@qub.ac.uk

piston's positional displacement, resulting in the air flowing into the soft robotics body [12]. In this work, the control variable is piston displacement to regulate the pressure. Zhang et al. developed a soft worm-like robot with five degrees of freedom driven pneumatically by an air pump for positive pressure and a sucking module for negative pressure [13]. Another work by Tolley et al. investigates two miniature air compressors (MAC) and six valves controlled by a microcontroller to actuate a pneumatically powered, untethered soft robotic [14]. In this work, the MAC will provide a constant rate of pressurized air while valves actuate the soft robot by switching the input between MAC and atmospheric pressure. This setup has the advantage of using valves while keeping the MAC at a constant rate of air. However, it doesn't vary the internal pressure for different bending configurations. A low-cost alternative is designed by Oguntosin et al. by using an air pump and two valves for air supply and exhaust [15]. The pump can be controlled by varying the pulse width modulation (PWM) signal from the microcontroller while the valves regulate the air supply and discharge air to the atmosphere. This system is modifiable using different pumps and valves, although it is limited to only one output channel.

The control of a pneumatic-based soft robot requires the delivery of pressure or fluid volume needed to reach the desired movement [11]. Pressure control is the system's low-level control in the actuator space [16]. Open loop control for a pneumatic-based soft robot requires modeling of the system to convey the pressure needed inside the soft robot. However, without a feedback mechanism, the open-loop control cannot indicate the attainment of the desired pressure and correct errors when a disturbance occurs. Establishing the sensor in closed-loop control provides feedback to correct errors because of unpredictable dynamics or disturbances. A pressure or flow sensor can provide the physical parameter state for a pneumatic-

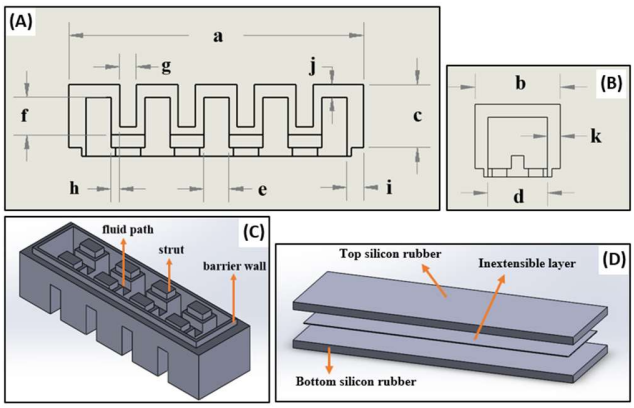

Fig. 1. Design of PneuNets platform. The 2D extensible layer design seen from (A) front longitudinal section and (B) side longitudinal section. (C) Bottom view of the 3D extensible layer design. (D) Structure of inextensible layer. Top silicon rubber was attached to the strut and barrier wall structures.

based soft robot. Gillespie et al. elaborated on the pressure sensors as feedback of a pneumatic soft robot platform called Grub in a Model Predictive Control to regulate the incoming airflow from the air sources [17]. Galloway et al. [18] employed the pressure and flow sensors as an evaluation platform system for the Fiber Reinforced Actuators. Zhang et al. m[13] demonstrated the application of pressure sensors in five air supply branches to control a soft worm-like robot with each branch that could be controlled independently.

This research highlights the fabrication of PneuNets, the effect of structural design modifications, and variations in the selection of materials in the inextensible layer in evaluating the movement of PneuNets. The pneumatic pump circuit used to drive the airflow to the PneuNets soft robot and the internal pressure control method were also evaluated. An input-tracking experiment was conducted to evaluate the performance of the pressure control system. To the best of our knowledge, the soft robotic with on-off and PI control systems is first presented in this article.

II. Materials And Methods

A. Reagents and Instruments

Tools and materials in the fabrication process are polylactic acid (PLA) filament 3D printer (Creality, Shenzhen, China), silicone rubber from Dragon Skin™ 10 medium (Smooth-On, Texas, US), vacuum pump Rocker 300 (Rocker, Kaohsiung, Taiwan). Image and video observation were performed using Smartphone Oppo A31 (Oppo, Dongguan, China). The actuator movement analysis was done using Kinovea under the GPL v2 license and Simulink (Mathworks, MA, USA) by placing the marker on the front side of the chambers.

TABLE I
PNEUNETS ACTUATOR DESIGN SIZE: VARIATION OF INNER CHAMBER WALL THICKNESS AND VARIATION OF INTER-CHAMBER DISTANCE

Code	Variation of inner chamber wall thickness			Variation of chamber distance		
	1 mm	2 mm	3 mm	2.5 mm	5 mm	10 mm
a	74	74	74	64	74	94
b	20	20	20	20	20	20
c	15	15	15	15	15	15
d	16	14	12	14	14	14
e	8	6	4	6	6	6
f	10	9	8	9	9	9
g	5	5	5	2.5	5	10
h	1	2	3	2	2	2
i	3	4	5	4	4	4
j	2	3	4	3	3	3
k	2	3	4	3	3	3

Components for developing a programmable pneumatic pump are microcontroller Arduino Mega 2560 (Arduino, Sommerville, United States), pressure sensor MPX53DP (NXP, Eindhoven, Netherlands), 6V DC Miniature Air Pump Motor (uxcell, Hong Kong China), and Miniature Solenoid Valve 2 Way 6V DC (uxcell, Hong Kong, China).

B. Pneumatic Networks (PneuNets)

The design comprises an extensible upper layer and an inextensible lower layer. In the extensible layer, there is a gap between the inner walls of each chamber. The inner wall of the chamber is thinner than the other exterior walls [19]. In the inextensible part, an additional layer functions as an unextended barrier layer [20]. The descriptions of the extensible layer structure shown in Figure 1A-B are: (a) extensible layer length, (b) extensible layer width, (c) extensible layer height, (d) chamber length, (e) chamber width, (f) chamber height, (g) distance between chambers, (h) inner chamber wall, (i) outer chamber wall, (j) upper chamber wall, and (k) side chamber wall. Figure 1C displays the bottom view of the extensible platform, and Figure 1D shows the structure of the inextensible layer sandwiched between silicon rubber layers. Based on these, we prepared eleven actuators for data collection and evaluation.

PneuNets move by bending due to increased internal pressure from airflow in the chamber. Adjacent chambers cause the inner walls to expand and the extensible layer to extend, resulting in a specific bending angle. At low air inflation rates, PneuNets form a circular shape. We optimized various parameters, including inner chamber wall thickness and inter-chamber distance, and evaluated the number of chambers and inextensible layer structure. Some aspects of the PneuNets structure were consistent, such as the extensible layer dimensions and the inextensible layer materials, which included wood-free paper and duplex cardboard. Table 1 summarizes the parameter variations, while Table S1 lists the optimization results. The three core materials were used for the inextensible structure: wood-free paper (houtvrij schrijfpapier /HVS), and white and brown duplex cardboard.

1) *Fabrication and evaluation*

Schematics of the fabrication process are summarized in Fig. S1 in the supplementary file. The PneuNets molds design was drawn using Solidworks (Dassault Systèmes, MA, USA). Final file files were exported to stereolithography (STL) format and fabricated by using a PLA 3D printer[19]–[23]. Two molds were produced. The first one was for the extensible layer and its cover, and the second one was for the inextensible layer. Next, silicone rubber, comprising polymer and hardener material, was mixed uniformly with a weight ratio of 1:1. Later, the silicone mixture was degassed to remove the air bubbles (4–5 min).

The silicone mixture was cast into the mold until the extensible layer was filled completely. Next, the inextensible layer was partially filled and covered by a duplex paper or cardboard. The casting was left for 4-5 hours for hardening. Subsequently, the silicone was peeled off. The additional silicone mixture was poured on top of a layer of duplex paper or cardboard on an inextensible layer until fully covered. Next, an extensible layer of silicone body was immersed in the mold sufficiently to create a closed joint with the inextensible layer.

Subsequently, the fabricated structure and its movement were visually inspected by taking photos and videos using a dark background for better contrast images. In addition, the testing protocols were done as described in [19]–[21], [24]. The retort stand held and clamped the actuator and pumping system. The black markers were attached to the front chambers to observe the actuator's motion and position. Finally, the first chamber was punctured using a syringe to open the inlet of air tubing from the pump system.

The quality control (QC) process involved leakage and actuation tests. Leakage tests were performed using colored water and air. Actuation tests were performed using Simulink. Air pump system was operated using PWM. The pressure values were measured, and the motion was visually recorded and analyzed to estimate the bending angle. Captured images were analyzed using Kinovea to obtain the coordinates position of markers. The bending positions were processed using mathematical equations from the three marker positions [25].

2) *Pneumatic Pumping system*

The pneumatic pump circuit design was constructed based on Oguntosin et al.[15]. This design comprises a pneumatic pump, solenoid valves, and a pressure sensor connected with tubes for an airflow path controlled by a microcontroller. The air pump supplies the compressed air, which is connected to an inlet solenoid valve. A T-connector provided two airflow paths, one connected with an exhaust valve and the other to the pressure sensor and the soft robotics body. A pressure sensor reading is sent to the microcontroller to measure air pressure. The system is programmed using a microcontroller for open and closed-loop control, with each sensor and actuator component of the system connected to a pin on the microcontroller. The actuators include a pneumatic pump controlled by a voltage signal as a PWM and solenoid valves controlled by a digital signal from the microcontroller.

Figure S2A (in the supplementary files) shows the scheme of the pneumatic pump system. A Simulink with Arduino support was used to control the open loop system and obtain the internal pressure. Mode of *Monitor & Tune* at Simulink was activated to read the sensing values in real-time, with the flexibility of

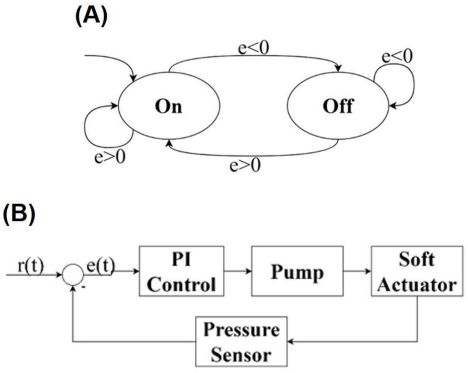

Fig. 2. (A) State diagram of on-off control. (B) PI control diagram.

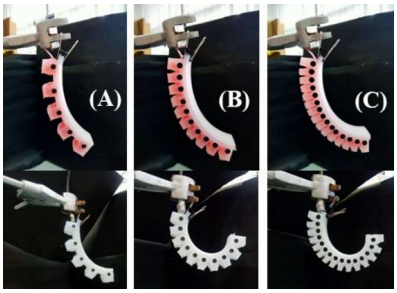

Fig. 3. Successful fabricated PneuNets structures with variations of total chambers: (A) 5, (B) 10, and (C) 15. The quality control using color water to observe fluid path. Air pressure movement on the platform show uniform delivery of air filling the actuator chambers.

parameter adjustment. The pump and valves were manually controlled using PWM. The sensing reading was calibrated using acquire and sum block, monitored in real-time using display block, and saved in Simulink workspace with a sampling time of 0.1 s. Figure S2B (in the supplementary files) shows the Simulink implementation.

In this current study, we apply two types of low-level controls: closed on-off system and PI control (Fig. 2A and B). On-off control accommodates the practical switching of the pump and valve. At the same time, PI control plays a significant role in error signal regulation in the control signal for the PWM input. In addition, pressure sensor monitoring is used as feedback in a closed-loop control system.

There are two states in the proposed closed-loop system: on-state for charging, and off-state for maintaining the last state. The pump is activated in the on-state, followed by the inlet valve opening. The air flows to the actuators and enhances the inner pressure. In the off state, the pump is deactivated, and the inlet valve is closed. Therefore, the inner pressure remains constant. The two states are determined based on the value of the error signal obtained: on-state with a positive error value and off-state with a negative error (Fig. 2A).

For the PI controller, an anti-windup compensation system is used to control the signal processing into the required voltage by the pump as a PWM signal. Anti-windup compensation keeps the control signal value within the desired PWM signal range and avoids integral windup. PWM signal is controlled at the operating region for the system (Fig. 2B). Determination of PI parameters is done using the model obtained from the system identification. The system model is represented as a transfer function equation, with the pressure value as the output and the normalised PWM value as the input. System identification takes data for random signal input with value changes every 20 s. A random signal was used to get an input within the range, while a time of 20 s allowed sufficient time for system stabilization The signal input was normalized PWM in the operating area; therefore, the value range becomes 0 and 1. The pressure sensing output was also filtered with a low-pass filter to reduce noise for system identification in the Simulink System Identification Tool. This identification system process utilizes the transfer function and enters the desired pole and zero values. Several models with different configurations of polar and zero values were derived, and the best-fit value was selected among the models.

III. Results and Discussion

A. PneuNets fabrication challenges

The major challenges in the PneuNets fabrication are the clogged and leakage air path. A clogged actuator reduces the uniformity of the airflow and the actuation response. The first failure occurred because of the fluid path and the silicon-enclosed chamber, as shown in Figure S3 (in the supplementary files). This clogged structure could be overcome by avoiding the overcasting of the top silicone with a height of slightly less than 2 mm, while the bottom silicone and the inextensible layer heights were 2 mm (Figure 1C-D). Leakage structure is another defect in the extensible part, such as a hole (Figure S3C). The primary source of the whole defect is the air bubbles during the silicone casting. Therefore, the degassing protocols and gentle casting are critical to obtain a uniform and solid polymer structure.

TABLE II
System Identification for PWM-Pressure Model.

Pole	Zero	Training Fit (%)	Validation 1 Fit (%)	Validation 2 Fit (%)
2	1	54.49	53.41	47.54
3	1	-39.31	-42.16	-45.73
3	2	72.95	69.99	64.11
4	1	63.52	56.93	59.53
4	2	73.55	70.06	64.45
4	3	19.54	16.92	13.75

Figure 3 demonstrates the successful PneuNets fabrication reflected in the test with colored water for validation and the fluid path and chamber could flow perfectly without clogged airflow. The entire actuator chamber could be expanded uniformly based on testing with an air pump. Eleven PneuNets structures with four-parameter variations were then tested for reproducibility production. The supplementary video SV1 shows the mechanism of the clogging reliability test using coloured water.

B. Pumping System Evaluation

A closed system testing using a soft robotic body was conducted to evaluate the pump circuit characteristics and performance. First, we tested the circuit for zero input conditions (Figure S4A in the supplementary file). At this stage, we observed the pressure sensor reading with no air supplied by the pump. The PWM values connected to the pump would have zero, while all valves would have to be open. The result shows the pressure measured at around 0 Pa with a maximum noise of less than 400 Pa. With this outcome, the pressure sensor was acceptable for measuring internal pressure. Next, we conducted a reading of sensor pressure for an increasing step input with a step time of 5 s. We set the pump PWM input to increase at 5s automatically and incrementally in SIMULINK. Figure S4B presents the pressure measurement result for increasing step PWM input, showing a correlation between PWM input and internal pressure in the operating region. A dead zone nonlinearity was seen before the pressure sensor read the

internal pressure change. In the operating region, the internal pressure increased gradually along with the increase in PWM signal value. This finding indicates the capability of the system to generate the internal air pressure needed to actuate a soft robotic system. However, the pressure value oscillated with a range of about ±2 kPa and a frequency of about 1.2 rad/s. Qualitatively, the oscillation occurred when the pump stopped delivering compressed air, causing the soft body to deflate and then restart, and the soft body expanded. The pressure in the system followed the expansion and deflation of the soft body, hence, the pressure oscillations obtained. This indicates the limitation of the air pump in maintaining the internal pressure because of the load given to the motor in the pump, which causes the pump to stop and go repeatedly. The average pressure data after 20 kPa yielded the pressure values at relatively the same range as 21-24 kPa. This was because of the limited sensor in the air pump system with a maximum ability to detect the pressure of around 22 kPa with a saturation value of pressure between 20-22 kPa.

Table 2 summarises the results of the models derived from system identification. Among those results, the model representation with four poles and two zeros produces the best fit.

$$G_L(s) = \frac{2644s^2 + 378.3s + 0.09105}{s^4 + 0.8557s^3 + 0.3971s^2 + 0.04481s + 3.215} \quad (1)$$

Model simplification was done by eliminating two pairs of adjacent poles and zero values. Thus, a second-order system model was obtained to represent the linear model for PWM pressure. The following was a reduced system model.

$$G_{reducted(s)} = \frac{161.1s + 2731}{s^2 + 0.7003s + 0.2882} \quad (2)$$

This linear model determined the PI control parameter to be 1.6078 x 10^{-4} for the proportional constant and 4.8022 x 10^{-5} for the integral constant. The system was given a pressure reference input signal as a step, sinusoidal, and random signal for testing. The step signal was used to check the system's response when a reference input was given from an idle condition. Five-step signals were set from 18 kPa to 22 kPa with 1 kPa steps. Each signal was 20 s long with a 10 s delay. The sinusoidal signal was used to ensure the ability of the system to follow an input reference. The sinusoidal signal used had a frequency of π/30 rad/s, an amplitude of 5 kPa with an offset of 20 kPa, and was run for 3 min to produce three waves. Like a sinusoidal signal, a random signal was used to check the controller's ability to follow the input reference and maintain its value. Figures 4A-4C show the test results for step, sinusoidal, and random signal inputs.

For PI control, some oscillations occur between about ±2 kPa from the input reference, with some exceptions. The pump characteristic could not maintain the applied pressure, as previously described. With some exceptions, the pressure value

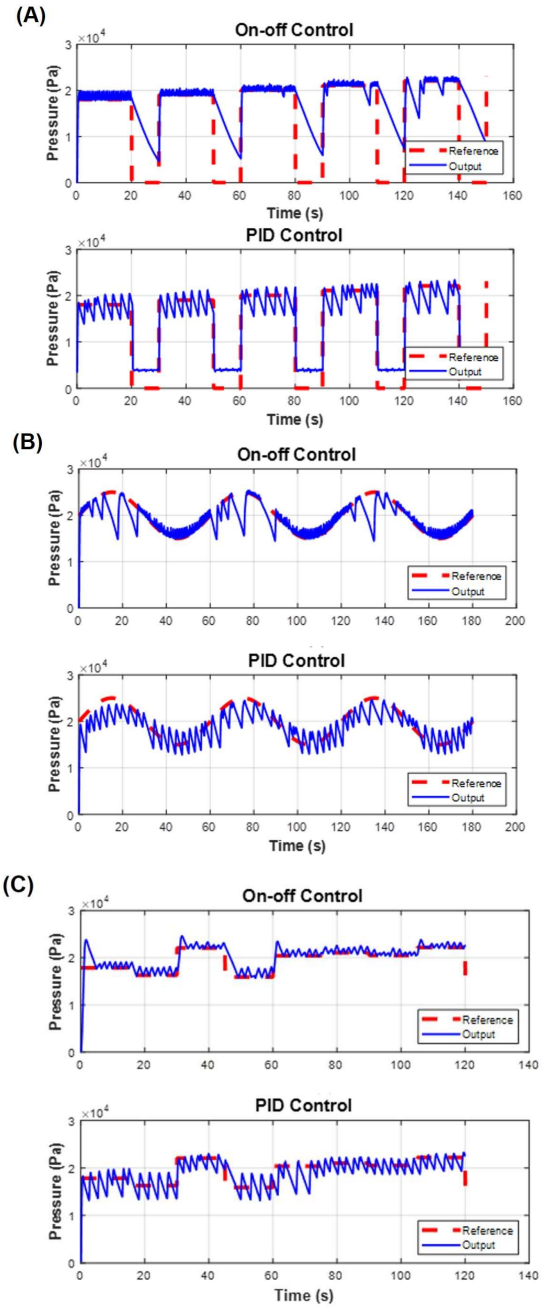

Fig. 4. PWM input pressure measurements: (A) Step input signal, (B) Sine wave input signal, (C) Random input signal.

was more than or equal to the input reference value for on-off control. The on-off and PI controls exhibited a pressure drop at some point, with the condition being more common at higher pressure values because the pump did not work constantly, and sometimes, there was a delay in the motor's rotation on the pump. The control signal was already at the upper limit of the PWM operating region at high pressure. Based on the results, the on-off control followed the input reference with a more minor error than the PI control. However, PI control was safer to use than on-off control because valves, as control, turned the pump off and on repeatedly and could trigger damage of the equipment significantly if the state change occurred in a short duration or chattering. The pump worked well within the

predetermined PWM value in the operating region for PI control.

C. PneuNets Bending test

The effect of the chamber wall thickness on the actuator bending angle is presented in Fig. 5. At relatively the same pressure value, different bending angles are produced. The thicker chamber wall produces a smaller bending angle at the same pressure. As the force is the product of surface area and pressure, in this actuator, the pressure comes from the air pressure, and the surface area is the area of the chamber side. Therefore, at relatively the same air pressure value, the magnitude of the compressive force is proportional to the surface area. Table S1 shows that the dimensions of the chamber with variations in the thickness of the inner chamber wall of 3 mm have the most diminutive chamber dimensions, and variations in the thickness of the inner chamber wall of 1 mm are the largest chamber dimensions. Based on the concept of force and pressure, the variation of the inner chamber wall thickness of 1 mm with the largest surface area of the chamber resulted in a most significant force than the other inner chamber wall thickness variations for the same pressure. Applying greater force to the extensible layer increases its elongation and bending angle. The thicker the chamber wall, the higher the force is required to expand the extensible and chamber parts, lowering the bending angle. The inner chamber wall is also essential because the inner chamber wall of an expanding chamber touches and pushes within the inner chamber wall of the other chamber, generating a larger bending angle.

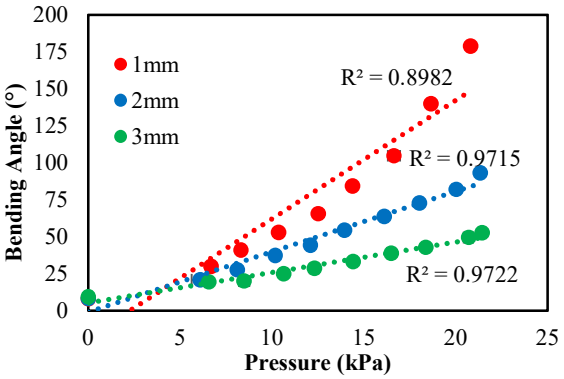

Fig. 5. The effects of bending angles as a function of pressure resulted by various thickness of inner chamber walls (*h* variable from Fig. 1).

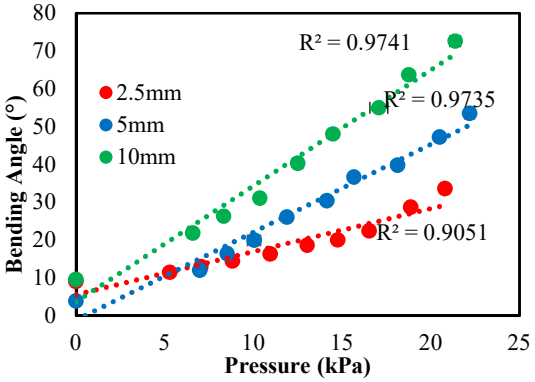

Fig. 6. The effects of bending angles as a function of pressure resulted by various distance between chambers (*g* variable from Fig. 1).

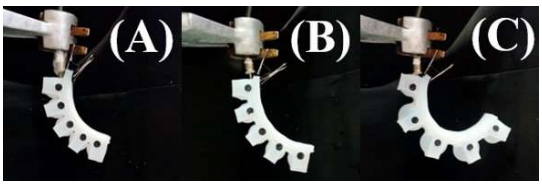

Fig. 7. The bending of PneuNets at the maximum capacity of the actuator pump varies distances between chambers (A) 2.5mm, (B) 5mm, and (C) 10mm.

1) *Distance between chambers*

The effect of the inter-chamber distance on the actuator bending angle is displayed in Fig. 6. The farther inter-chamber distance resulted in a bigger bending angle at the same pressure. However, this result did not follow the initial hypothesis. Other studies have also stated that the smaller the inter-chamber distance, the higher the bending angle produced [8]. Therefore, if the distance between chambers was getting smaller, then the inner wall of one chamber and the inner wall of another chamber touch and push each other, producing a larger bending angle.

The distance variations between PneuNets chambers include the same width and height but different lengths. As listed in Table S1, the design variations in the 2.5 mm, 5 mm, and 10 mm inter-chamber distances with the exact chamber dimensions affect the length of the extensible layers of 64 mm, 74 mm, and 94 mm. This design did not hypothetically fall

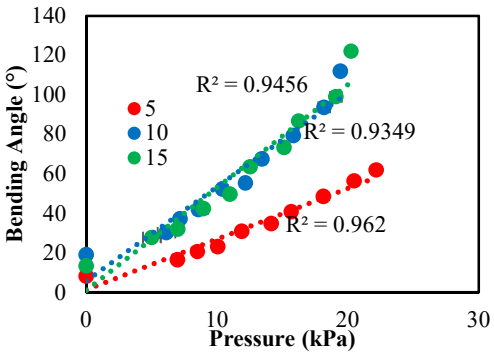

Fig. 8. The effects of bending angle of the actuators with different numbers of chamber as a function of pressure.

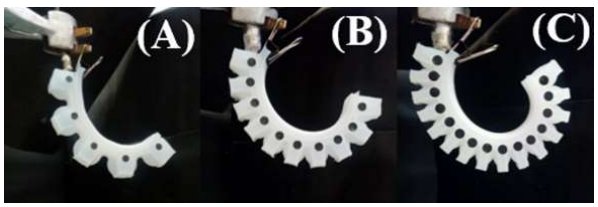

Fig. 9. The bending of PneuNets at the maximum capacity of the actuator pump with different number of chambers; (A) 5, (B) 10, and (C) 15.

within the results of the bending angle on the variation of parameters. It is proven in the moment of force, is equal to the force multiplied by the moment arm. The acting force raises due to air pressure and the surface area of the extensible layer and chamber. Because of the exact chamber dimensions, the resulting force was assumed to be the same at the same pressure. Because of the difference in the actuator length (with the same number of chambers and arrangement), the moment of force acting on the actuator with the most extended size increases because of the higher moment arm. As a result, the bending angle actuators are significantly produced with extended sizes, as shown in Fig. 7. The longer PneuNets actuators with the same number and placement of chambers result in a higher bending angle produced. The more chambers with the same actuator's length reinforce the increment of the bending angle with the actuator dimensions shown in Table S1 (in the supplementary files) under the same pressure. Figure 8 depicts the impacts of the chamber's number on the bending angle of the actuator. More chambers with the same actuator length produce a higher bending angle with the actuator dimensions shown in Table S1 (in the supplementary files) at the same pressure. The chamber in actuator PneuNets plays a crucial part in the extensible layer that affects its bending. More chambers increase the actuator's bending angle, which is caused by the number of chambers and the friction from the inner chamber walls that push each other. It is noticed that more chambers with smaller inter-chamber distances trigger the bending angle increment because of the more intense thrust within the inner chamber walls. Fig. 9 shows the bending angle of the actuator in the actuator test with variations in the number of chambers 5, 10, and 15 at the maximum capacity of the air pump, respectively, which are 136.94°, 17 7.33°, and 221.67°. The supplementary video SV2 demonstrates the bending mechanism of 10 chambers PneuNets actuator.

The effect of material selection on an inextensible layer with the same design size as listed in Table S2 on the bending angle is presented in Figure 10. Based on the measurements and calculations presented in Table S2, the highest grammage value was a brown duplex, and the lowest was HVS. Identification of a paper was done through its grammage value. The thickness defines the stiffness of the paper. Also, the higher paper grammage value on the inextensible layer makes it difficult to bend to lower the bending angle. As a summary, we list several related research related to soft robotics in Table III.

IV. Conclusions

PneuNets soft robotic has been fabricated successfully and controlled using simple on-off based on the pressure state feedback and PI configuration based on a linear model derived from system identification in a predetermined operating region. The bending angle performance is highly tunable with several parameters, such as the chamber spacer, the thickness of the chamber wall, the number of chambers, and the grammage of the materials for the actuators. For input tracking performance, the on-off control shows track input with better error performance than the PI control, with the PI control producing an oscillation along the input reference of about ±2 kPa. However, a PI control offers a safer performance compared to the on-off controller to prevent damage to the circuit during high-frequency switching. For future works, the high-level control system paired with this proposed PneuNets system is proposed to fully control the soft robot.

TABLE III
COMPARATIVE STUDIES OF SOFT ROBOTICS

Soft body	Motoric	Sensing	Control	Finding	Ref
PneuNets	Pneumatic system	Flex	PID variance	Sinusoid signal (f: 0.5 Hz) with PID *piecewise* and *fuzzy* optimally performed	[26]
PneuNets	Valve	Pressure, Flex	PID variance	Target angle with mean error of 0.752° with SD 2.09°	[27]
FEA line segments	Pneumatic cylinders	Camera	PI-PID cascade	Position accuracy 0.71 cm; Rotation accuracy 1.1°	[28]
FEA cylinder segment	Pneumatic cylinders	Camera	PID	Optimum error when norm L_2 <0.2 with f: 2.8 rad/s and amplitude 0.24 rad	[29]
FEA cylinder segment	Pump dan valve	Flex	PI	Max bending angle error 1.08°	[30]
Fiber Reinforced Actuator	Pump dan valve	Magnetic	*Sliding mode Control*	Response time 0.2s (0% *overshoot)* for step response, undelayed response f_{max}: 1kHz	[31]
Pneumatics segment based on cloth	Pump dan valve	Pressure, IMU	MPC	2-state MPC resulted in an average *overshoot* of 24.408% (7.3°). 4-state MPC resulted in an average *overshoot* of 2.587% (<0.78°).	[32]
Pneumatic curling rubber actuator	Compressor and electro-pneumatic regulator	Camera	Support Vector Regression (SVR)	Computing time: 23.5 with a fit ratio of 83.5% for the 1437 dataset.	[33]
Pneumatic curling rubber actuator	Compressor and electro-pneumatic regulator	Camera	SVR	Able to perform sensorless feedback system	[34]
3-DOF soft actuator	Compressor and electro-pneumatic regulator	Camera	MSVR inverse model	Tip-position coordinates followed target values with limited errors	[35]
PneuNets	Pump and valve	Pressure	On-Off, PI	Bending angle up to 120° (15 chambers)	This work

APPENDIX

The supplementary files contain figures, table, and videos that are separated from the main manuscript.

ACKNOWLEDGMENT

This work was partly supported by the School of Electrical Engineering and Informatics, Bandung Institute of Technology, Indonesia. Yulyan Wahyu Hadi and Basilius Agung Yason Sunarya contribute equally to this work.

REFERENCES

[1] H. Le Ferrand, "Robotics: Science preceding science fiction," *MRS Bull*, vol. 44, no. 4, pp. 295–301, Apr. 2019, doi: 10.1557/mrs.2019.68.

[2] G. Alici, "Softer is harder: What differentiates soft robotics from hard robotics?," in *MRS Advances*, 2018, vol. 3, no. 28. doi: 10.1557/adv.2018.159.

[3] G. M. Whitesides, "Soft-Robotik," *Angewandte Chemie*, vol. 130, no. 16, pp. 4336–4353, Apr. 2018, doi: 10.1002/ange.201800907.

[4] M. Cianchetti, C. Laschi, A. Menciassi, and P. Dario, "Biomedical applications of soft robotics," *Nat Rev Mater*, vol. 3, no. 6, pp. 143–153, 2018, doi: 10.1038/s41578-018-0022-y.

[5] D. Rus and M. T. Tolley, "Design, fabrication and control of soft robots," *Nature*, vol. 521, no. 7553. Nature Publishing Group, pp. 467–475, May 27, 2015. doi: 10.1038/nature14543.

[6] C. Lee *et al.*, "Soft robot review," *International Journal of Control, Automation and Systems*, vol. 15, no. 1. Institute of Control, Robotics and Systems, pp. 3–15, Feb. 01, 2017. doi: 10.1007/s12555-016-0462-3.

[7] C. Laschi, B. Mazzolai, and M. Cianchetti, "Soft robotics: Technologies and systems pushing the boundaries of robot abilities," *Science Robotics*, vol. 1, no. 1. 2016. doi: 10.1126/scirobotics.aah3690.

[8] W. Hu, R. Mutlu, W. Li, and G. Alici, "A structural optimisation method for a soft pneumatic actuator," *Robotics*, vol. 7, no. 2, 2018, doi: 10.3390/robotics7020024.

[9] M. Manti, V. Cacucciolo, and M. Cianchetti, "Stiffening in soft robotics: A review of the state of the art," *IEEE Robot Autom Mag*, vol. 23, no. 3, 2016, doi: 10.1109/MRA.2016.2582718.

[10] J. Wang and A. Chortos, "Control Strategies for Soft Robot Systems," *Advanced Intelligent Systems*, vol. 4, no. 5, 2022, doi: 10.1002/aisy.202100165.

[11] P. Polygerinos *et al.*, "Soft Robotics: Review of Fluid-Driven Intrinsically Soft Devices; Manufacturing, Sensing, Control, and Applications in Human-Robot Interaction," *Advanced Engineering Materials*, vol. 19, no. 12. 2017. doi: 10.1002/adem.201700016.

[12] A. D. Marchese, K. Komorowski, C. D. Onal, and D. Rus, "Design and control of a soft and continuously deformable 2D robotic manipulation system," in *Proceedings - IEEE International Conference on Robotics and Automation*, 2014. doi: 10.1109/ICRA.2014.6907161.

[13] B. Zhang, Y. Fan, P. Yang, T. Cao, and H. Liao, "Worm-like soft robot for complicated tubular environments," *Soft Robotics*, vol. 6, no. 3. 2019. doi: 10.1089/soro.2018.0088.

[14] M. T. Tolley *et al.*, "A Resilient, Untethered Soft Robot," *Soft Robot*, vol. 1, no. 3, 2014, doi: 10.1089/soro.2014.0008.

[15] V. Oguntosin, S. J. Nasuto, and Y. Hayashi, "A compact low-cost electronic hardware design for actuating soft robots," *International Journal of Simulation: Systems, Science and Technology*, vol. 16, no. 3, 2015, doi: 10.5013/IJSSST.a.16.03.06.

[16] T. George Thuruthel, Y. Ansari, E. Falotico, and C. Laschi, "Control Strategies for Soft Robotic Manipulators: A Survey," *Soft Robotics*, vol. 5, no. 2. 2018. doi: 10.1089/soro.2017.0007.

[17] M. T. Gillespie, C. M. Best, and M. D. Killpack, "Simultaneous position and stiffness control for an inflatable soft robot," in *Proceedings - IEEE International Conference on Robotics and Automation*, 2016, vol. 2016-June. doi: 10.1109/ICRA.2016.7487240.

[18] K. C. Galloway, P. Polygerinos, C. J. Walsh, and R. J. Wood, "Mechanically programmable bend radius for fiber-reinforced soft actuators," in *2013 16th International Conference on Advanced Robotics, ICAR 2013*, 2013. doi: 10.1109/ICAR.2013.6766586.

[19] B. Mosadegh *et al.*, "Pneumatic networks for soft robotics that actuate rapidly," *Adv Funct Mater*, vol. 24, no. 15, 2014, doi: 10.1002/adfm.201303288.

[20] P. Polygerinos *et al.*, "Towards a soft pneumatic glove for hand rehabilitation," in *IEEE International Conference on Intelligent Robots and Systems*, 2013. doi: 10.1109/IROS.2013.6696549.

[21] M. Luo, W. Tao, F. Chen, T. K. Khuu, S. Ozel, and C. D. Onal, "Design improvements and dynamic characterization on fluidic elastomer actuators for a soft robotic snake," in *IEEE Conference on Technologies for Practical Robot Applications, TePRA*, 2014. doi: 10.1109/TePRA.2014.6869154.

[22] L. Wei *et al.*, "3D-printed low-cost fabrication and facile integration of flexible epidermal microfluidics platform," *Sens Actuators B Chem*, vol. 353, no. November 2021, p. 131085, 2022, doi: 10.1016/j.snb.2021.131085.

[23] A. M. E. Arefin, N. R. Khatri, N. Kulkarni, and P. F. Egan, "Polymer 3D Printing Review: Materials, Process, and Design Strategies for Medical Applications," *Polymers (Basel)*, vol. 13, no. 9, p. 1499, 2021.

[24] Y. Li, Y. Chen, T. Ren, Y. Li, and S. H. Choi, "Precharged Pneumatic Soft Actuators and Their Applications to Untethered Soft Robots," *Soft Robot*, vol. 5, no. 5, 2018, doi: 10.1089/soro.2017.0090.

[25] J. Auysakul, N. Vittayaphadung, S. Gonsrang, and P. Smithmaitrie, "Bending angle effect of the cross-section ratio for a soft pneumatic actuator," *International Journal of Mechanical Engineering and Robotics Research*, vol. 9, no. 3, pp. 366–370, 2020, doi: 10.18178/ijmerr.9.3.366-370.

[26] A. H. Khan, Z. Shao, S. Li, Q. Wang, and N. Guan, "Which is the best PID variant for pneumatic soft robots? an experimental study," *IEEE/CAA Journal of Automatica Sinica*, vol. 7, no. 2, pp. 451–460, Mar. 2020, doi: 10.1109/JAS.2020.1003045.

[27] K. Elgeneidy, N. Lohse, and M. Jackson, "Bending angle prediction and control of soft pneumatic actuators with embedded flex sensors – A data-driven approach," *Mechatronics*, vol. 50, pp. 234–247, Apr. 2018, doi: 10.1016/J.MECHATRONICS.2017.10.005.

[28] A. D. Marchese, K. Komorowski, C. D. Onal, and D. Rus, "Design and control of a soft and continuously deformable 2D robotic manipulation system," *Proc IEEE Int Conf Robot Autom*, pp. 2189–2196, Sep. 2014, doi: 10.1109/ICRA.2014.6907161.

[29] C. Della Santina, R. K. Katzschmann, A. Bicchi, and D. Rus, "Dynamic control of soft robots interacting with the environment," *2018 IEEE International Conference on Soft Robotics, RoboSoft 2018*, pp. 46–53, Jul. 2018, doi: 10.1109/ROBOSOFT.2018.8404895.

[30] G. Gerboni, A. Diodato, G. Ciuti, M. Cianchetti, and A. Menciassi, "Feedback Control of Soft Robot Actuators via Commercial Flex Bend Sensors," *IEEE/ASME Transactions on Mechatronics*, vol. 22, no. 4, pp. 1881–1888, Aug. 2017, doi: 10.1109/TMECH.2017.2699677.

[31] M. Luo *et al.*, "Toward Modular Soft Robotics: Proprioceptive Curvature Sensing and Sliding-Mode Control of Soft Bidirectional Bending Modules," *https://home.liebertpub.com/soro*, vol. 4, no. 2, pp. 117–125, Jun. 2017, doi: 10.1089/SORO.2016.0041.

[32] C. M. Best, M. T. Gillespie, P. Hyatt, L. Rupert, V. Sherrod, and M. D. Killpack, "A New Soft Robot Control Method: Using Model Predictive Control for a Pneumatically Actuated Humanoid," *IEEE Robot Autom Mag*, vol. 23, no. 3, pp. 75–84, Sep. 2016, doi: 10.1109/MRA.2016.2580591.

[33] K. Fujita, M. Deng, and S. Wakimoto, "A Miniature Pneumatic Bending Rubber Actuator Controlled by Using the PSO-SVR-Based Motion Estimation Method with the Generalized Gaussian Kernel," *Actuators*, vol. 6, no. 1, 2017, doi: 10.3390/act6010006.

[34] M. Deng and T. Kawashima, "Adaptive Nonlinear Sensorless Control for an Uncertain Miniature Pneumatic Curling Rubber Actuator Using Passivity and Robust Right Coprime Factorization," *IEEE Transactions on Control Systems Technology*, vol. 24, no. 1, pp. 318–324, 2016, doi: 10.1109/TCST.2015.2424853.

[35] T. Usami and M. Deng, "Applying an MSVR Method to Forecast a Three-Degree-of-Freedom Soft Actuator for a Nonlinear Position Control System: Simulation and Experiments," *IEEE Syst Man Cybern Mag*, vol. 8, no. 3, pp. 61–69, 2022, doi: 10.1109/MSMC.2022.3153747.